

This item is the archived peer-reviewed author-version of:

Aggregation of purple bacteria in an upflow photobioreactor to facilitate solid/liquid separation : impact of organic loading rate, hydraulic retention time and water composition

Reference:

Blansaer Naïm, Alloul Abbas, Verstraete Willy, Vlaeminck Siegfried, Smets Barth F..- Aggregation of purple bacteria in an upflow photobioreactor to facilitate solid/liquid separation : impact of organic loading rate, hydraulic retention time and water composition
Bioresource technology - ISSN 1873-2976 - 348(2022), 126806
Full text (Publisher's DOI): <https://doi.org/10.1016/J.BIORTECH.2022.126806>
To cite this reference: <https://hdl.handle.net/10067/1858430151162165141>

1 **Aggregation of purple bacteria in an upflow photobioreactor to facilitate solid/liquid**
2 **separation: Impact of organic loading rate, hydraulic retention time and water**
3 **composition**

4
5 **Naïm Blansaer^{1**}, Abbas Alloul^{1**}, Willy Verstraete², Siegfried E. Vlaeminck¹ and**
6 **Barth F. Smets^{3*}**

7
8 ¹ Research Group of Sustainable Energy, Air and Water Technology, Department of
9 Bioscience Engineering, University of Antwerp, Groenenborgerlaan 171, 2020 Antwerpen,
10 Belgium

11 ² Center for Microbial Ecology and Technology, Faculty of Bioscience Engineering, Ghent
12 University, Coupure Links 653, 9000 Gent, Belgium

13 ³ Department of Environmental Engineering, Technical University of Denmark, Kongens
14 Lyngby 28000, Denmark

15

16 * Corresponding author: Barth F. Smets, bfsm@env.dtu.dk

17 ** Equally contributed as first authors

18 **Abstract**

19 Purple non-sulfur bacteria (PNSB) form an interesting group of microbes for resource
20 recovery from wastewater. Solid/liquid separation is key for biomass and value-added
21 products recovery, yet insights into PNSB aggregation are thus far limited. This study
22 explored the effects of organic loading rate (OLR), hydraulic retention time (HRT) and water
23 composition on the aggregation of *Rhodobacter capsulatus* in an anaerobic upflow
24 photobioreactor. Between 2.0-14.6 gCOD/(L.d), the optimal OLR for aggregation was 6.1
25 gCOD/(L.d), resulting in a sedimentation flux of 5.9 kgTSS/(m².h). For HRT tested between
26 0.04-1.00 d, disaggregation occurred at the relatively long HRT (1 d), possibly due to
27 accumulation of thus far unidentified heat-labile metabolites. Chemical oxygen demand
28 (COD) to nitrogen (6-35 gCOD/gN) and the nitrogen source (ammonium vs. glutamate) also
29 impacted aggregation, highlighting the importance of the specific wastewater type and its
30 pre-treatment. These novel insights to improve purple biomass separation pave the way for
31 cost-efficient PNSB applications.

32

33 **Keywords:** nutrient recovery, purple phototrophic bacteria, granular sludge, flocculation,
34 granulation

35

36 **1 Introduction**

37 Purple non-sulfur bacteria (PNSB), a major group of purple phototrophic bacteria, show
38 potential for resource recovery from wastewater, process water, sidestreams and
39 byproducts containing biodegradable organics and nutrients (Alloul et al., 2018;
40 Capson-Tojo et al., 2020; Monroy and Buitrón, 2020). These microbes are
41 metabolically versatile and can use a wide variety of carbon and nitrogen sources, both
42 phototrophically as well as chemotrophically (Imhoff, 2006). In resource recovery,
43 PNSB are typically exploited in photohetero- or -mixotrophic mode where they use
44 light as energy source and organics optionally in combination with inorganic carbon as
45 carbon source(s). Different value-added products have been investigated for resource
46 recovery by PNSB such as microbial protein, fertilizers and polyhydroxyalkanoates
47 (Alloul et al., 2021; Capson-Tojo et al., 2020; Sakarika et al., 2020). Research to
48 efficiently harvest PNSB-rich biomass is, however, limited. Gravitational methods are
49 typically more cost-efficient than membrane separation. In wastewater treatment,
50 gravitational methods can reduce total costs by 38-53% compared to membrane-based
51 systems (Bertanza et al., 2017). Gravitational solid/liquid separating within a feasible
52 amount of time relies on (bio)aggregation of cells into flocs and granules. Aggregation
53 of biomass consists of different mechanisms, where repulsion between cells is to
54 overcome. Polyvalent cations play an important role in the bridging of microbial cells,
55 whereas extracellular polymeric substances allow cells to coagulate by changing the cell
56 surface hydrophobicity, cell surface charge or serve as a microbial glue (Gao et al.,
57 2011; Liu et al., 2003; Suresh et al., 2018). For aerobic activated sludge, the growth of
58 filamentous bacteria helps cells to aggregate as well, forming a backbone for
59 microorganisms to attach to (Verstraete and van Vaerenbergh, 1986). Floc formation or

60 flocculation can be realized by applying a selective pressure on the microbial
61 community through washout of poorly settling biomass (e.g. upflow reactors or
62 sequencing batch reactors), addition of chemical coagulants (e.g. Ca^{2+} , Al^{3+}), adjusting
63 the feeding strategy or changing the chemical oxygen demand to nitrogen (COD/N)
64 ratio in the feed (Suresh et al., 2018). Granulation of the biomass can be achieved
65 through applying increased hydrodynamic shear, regulating the feeding strategy or
66 changing the organic load rate (OLR) in a sequencing batch reactor or upflow reactor
67 systems, such as upflow anaerobic sludge blanket (UASB) reactors (de Sousa
68 Rollemberg et al., 2018; Lim and Kim, 2014).

69 Limited literature can be found on the aggregation of PNSB biomass in
70 bioreactors, and up to now, only two biotechnological approaches have been explored.
71 Washing out non-settling biomass in a sequencing batch photobioreactor after each run,
72 with increasing OLR from 0.2 to 1.3 gCOD/(L.d) and decreasing hydraulic retention
73 time (HRT) from 2 d to 0.67 d, lead to accumulation of aggregating biomass, forming
74 granules with a sedimentation flux of 4.7 kgVSS/(m².h) (Cerruti et al., 2020). Similarly,
75 continuous upflow photobioreactors have proven to be successful for PNSB
76 aggregation. The work by Driessens et al. (1987), for example, achieved aggregation of
77 PNSB-rich sludge with a sedimentation flux of 1-2 kg/(m².h). More recently, Stegman
78 et al. (2021) obtained PNSB granules in an upflow reactor testing different upflow rates
79 (2-9 m/h), forming granules with a sludge volume index (SVI₃₀) of 10 mL/g and
80 average settling velocities above 30 m/h. High COD and nitrogen removal efficiencies
81 around 60-90% have been achieved for all these systems. Optimization is, however, still
82 required to reach the effluent discharge limits of 125 mgCOD/L and 15 mgN/L (CEC,
83 1991). A systematic understanding of the effect of operational tools and wastewater

84 composition, for example, COD/N ratio and nitrogen source, on the aggregation of
85 PNSB-rich biomass are, however, still missing, although these parameters influence
86 aggregation (Suresh et al., 2018).

87 The main goal of this research was to acquire a systematic understanding of the
88 effect of operational tools and wastewater composition on the aggregation of PNSB-rich
89 biomass. The aggregation mechanism or the structure of the aggregates were not
90 studied, yet are also crucial for process control. In terms of aggregate size, an average
91 diameter of around 100 μm has been observed for PNSB granules and a uniform interior
92 structure with a community dominated by purple bacteria has been detected (Cerruti et
93 al., 2020; Stegman et al., 2021). The research on the structure of PNSB aggregates and
94 the mechanism of aggregation remains nevertheless limited compared to other fields
95 such as aerobic sludge flocculation or anaerobic granulates. For flocculation, for
96 example, it has been shown that a properly balanced ratio of floc formers and
97 filamentous microorganisms is required for good settling biomass. The temperature has
98 also been shown to influence flocculation through a change in filaments population or
99 surface charge (Krishna and van Loosdrecht, 1999; Morgan-Sagastume and Allen,
100 2005). Divalent cations are also key for both granular and floccular sludge as Ca_2^+ ,
101 Mg_2^+ and Fe_3^+ will bridge negatively charged functional groups within the extracellular
102 polymeric substances and contribute to adhesion (Gao et al., 2011; Suresh et al., 2018;
103 Tiwari et al., 2006). These mechanistic insights are also important for PNSB. Follow-up
104 research is, therefore, necessary to effectively characterize PNSB aggregates in terms of
105 size distribution, extracellular polymeric substance, and spatial organization (e.g.
106 fluorescence in situ hybridization). Combined with tests on the ionic matrix (mono- and

107 bivalent ratio) and shear, it can provide a deeper understanding of the mechanisms of
108 PNSB aggregation.

109 **2 Materials and methods**

110 **2.1 Inoculum and medium composition**

111 *Rhodobacter capsulatus* ATCC 23782 (available at the American Type Culture
112 Collection), selected as a model organism for PNSB, was precultivated in closed test
113 tubes of 24 mL under axenic conditions with a light intensity of 85-100 $\mu\text{E}/(\text{m}^2\cdot\text{s})$ on
114 synthetic wastewater based on Segers and Verstraete (1983), containing calcium lactate
115 as carbon source (2.4 g/L, hence 2.4 gCOD/L) and sodium glutamate (1.3 g/L, hence
116 0.12 g N/L and 1.2 g COD/L) as a nitrogen source, and a relatively high dose of
117 HKPO_4^- to act as pH buffer (0.3 gP/L) at a pH of 6.8, enriched with 1 mL of a vitamin
118 solution per liter of medium, containing nicotinic acid (0.1 g/L), biotin (0.015 g/L) and
119 thiamine-HCl 1.0 (g/L). Multiple batch growth tests were conducted with *Rb.*
120 *capsulatus* at different COD concentrations (0.1, 0.2, 0.4, 0.5, 0.7, 0.8, 1.1, 1.3, 2.5, 4.9
121 and 9.7 gCOD/L) to characterize the inoculum and derive the Monod kinetics (see
122 supplementary material).

123 For reactor operations, the nitrogen source was changed to ammonium sulfate,
124 except when glutamate was used to investigate the influence of the nitrogen source
125 (section 3.2.2). In the batch reactor, the medium was sterilized to explore the influence
126 of PNSB metabolites on aggregation (section 3.1.2), while for the continuous upflow
127 reactor, the medium was not sterilized to mimic wastewater conditions.

128 **2.2 Reactor set-ups and operation**

129 The batch reactor consisted out of cylindrical tubes with an inner diameter of 3.5
130 cm and a volume of 400 mL. All parts of the reactor were autoclaved at 121°C with an
131 overpressure of 1 atm for 20 min and procedures were conducted in the laminar flow to
132 work axenically. The reactor was inoculated at 5 %v/v with axenic inoculum (grown for
133 2-3 d) and the headspace was flushed for 2 minutes with argon to create an anaerobic
134 environment. The reactor was operated at a temperature of 36 to 38 °C and illuminated
135 with Gro-Lux Fluorescent lamps F40/T12 (Sylvania), supplemented with spotlights of
136 150 W to reach a light intensity between 85 and 100 $\mu\text{E}/(\text{m}^2.\text{s})$.

137 The continuous reactor, illustrated in Figure 1, had an inner diameter of 3.5 cm,
138 an illuminated volume of 440 mL and a decanter with an inner diameter of 9.5 cm on
139 top. The carbon- and nitrogen-containing media were dosed separately with peristaltic
140 pumps to minimize microbial contamination and bioconversion in the feed. Feeding was
141 discontinuous for 2 times 5 min every hour yielding flow rates of 0.44, 3.1, 4.4 and 10.6
142 L/d (corresponding to HRT of 1, 0.3, 0.1 and 0.04 d, respectively). HRT was calculated
143 using the following equation: $\text{HRT} = V_{\text{reactor}}/Q_{\text{influent}}$, with V_{reactor} the volume of the
144 reactor and Q_{influent} the flow rate of the influent. The internal recirculation yielded
145 upflow rates in the reactor and the decanter of 1 m/h and 0.15 m/h, respectively. The
146 reactor was consistently inoculated at 5 %v/v with axenic inoculum of *Rb. capsulatus*
147 (grown for 3 d, more information on growth characteristics available in supplementary
148 material) and illuminated with Gro-Lux Fluorescent lamps F40/T12 (Sylvania),
149 supplemented with spotlights of 150 W. Light intensities were between 150-170
150 $\mu\text{E}/(\text{m}^2.\text{s})$ because it was expected that aggregation will result in higher biomass
151 concentrations and thus lower light penetration compared to the batch test (85-100
152 $\mu\text{E}/(\text{m}^2.\text{s})$).

153 Before testing different conditions, the reactor was operated at an OLR of 6.1
154 gCOD/(L.d), an HRT of 0.1 d and a COD/N ratio of 12 gCOD/gN to achieve
155 aggregation, based on previous research of Driessens et al. (1987). First, the influence
156 of OLR, coupled to HRT (section 3.1.1), was examined by operating the reactor in four
157 subsequent phases: (i) HRT 0.1 d (OLR 6.1 gCOD/(L.d)), (ii) HRT 0.04 d (OLR 14.6
158 gCOD/(L.d)), (iii) HRT 0.1 d (OLR 6.1 gCOD/(L.d)), and (iv) HRT 0.3 d (OLR 2.0
159 gCOD/(L.d)). The sedimentation flux was determined at HRT 0.04 and 0.1 d (no
160 aggregation was observed at HRT of 0.3 d) for different dilutions of biomass harvested
161 from the reactor.

162 To study the effect of metabolites accumulation at long HRT (1 d), aggregation
163 was first established at an HRT of 0.1 d in two separate photobioreactors. The HRT was
164 then increased to 1 d. When disaggregation occurred, tannic acid, an organic flocculant
165 used in wastewater treatment, was added to the feed at 10 mg/(L.d) to one
166 photobioreactor. In the photobioreactor without flocculant dosing, the medium in the
167 recirculation loop was pasteurized in flasks for 15 minutes at 60 °C, 60-65 °C, and 70-
168 80 °C.

169 To investigate the effect of accumulated metabolites, *Rb. capsulatus* was
170 axenically cultivated in batch (no aggregation was observed) for 2 to 4 d. The broth was
171 centrifuged at a relative g force of 20000g to separate the biomass and the supernatant.
172 Before feeding the supernatant to the reactor, it was enriched with carbon and nitrogen
173 to achieve an OLR of 12.2 gCOD/(L.d) and COD/N ratio of 12 gCOD/gN. Half of the
174 minerals (see section 2.1) were also added. To test the hypothesis of heat-labile
175 disaggregation metabolites, the supernatant was first autoclaved (section 3.1.2). The
176 reactor was operated at five subsequential phases, at an HRT of 0.1 d: (i) start-up phase

177 without the addition of supernatant, (ii) addition of supernatant of non-aggregated
178 axenic batch cultures grown for 3 to 4 d to study the effect of disaggregation
179 metabolites on PNSB aggregation, (iii) re-aggregation by stopping the addition of
180 supernatant, (iv) addition of autoclaved supernatant and (v) addition of non-autoclaved
181 supernatant of batch cultures grown for 2 to 3 d to examine the effect of lower
182 concentrations of the disaggregation metabolites.

183 To explore the influence of the influent COD/N ratio (section 3.2.1), two upflow
184 anaerobic photobioreactors were set up in parallel, both initially operated at a COD/N
185 ratio of 12 gCOD/gN and HRT of 0.1 d, based on Driessens et al. (1987). After 15 days,
186 the COD/N ratio was doubled to 24 gCOD/gN in one reactor and 6 gCOD/gN in the
187 other. The last experiment (section 3.2.2) had the objective to investigate the effect of
188 the nitrogen source, the nitrogen source was changed to glutamate, as a proxy for
189 organic nitrogen, after achieving aggregation in a startup phase with ammonium at a
190 COD/N ratio of 12 gCOD/gN. The reactor was operated in two phases with glutamate
191 as the nitrogen source: (i) at a COD/N ratio of 35 gCOD/gN and (ii) at 22 gCOD/gN.
192 The COD/N ratios for the experiment were based on the COD/N uptake ratios of PNSB
193 (16-20 gCOD/gN) (Hülßen et al., 2014). These COD/N uptake ratios are lower
194 compared to anaerobic digestion (57-140 gCOD/gN) because the fraction of incoming
195 COD that is converted to biomass is higher (0.5-1.0 vs. 0.01 gCOD_{biomass}/gCOD_{removed}
196 for anaerobic digestion), resulting in a higher N-need (Mata-Alvarez, 2003; Metcalf et
197 al., 1991). An overview of the different test conditions is presented in Table 1.

198 **2.3 Analytical procedures**

199 COD and NH₄⁺-N were determined according to standard procedures NBN T91-
200 201 and NBN T91-252, respectively. The biomass content, harvested directly from the
201 reactor (the biomass content in the recirculation vessels was negligible), was measured
202 after drying the sample at 105 °C (total suspended solids, TSS) and incineration at 650
203 °C for two hours (volatile suspended solids, VSS). Four biomass concentrations (100,
204 80, 60 and 40 %v/v) were tested in sedimentation cylinders of 50 mL to determine the
205 sedimentation flux according to Verstraete et al. (1984). This parameter was selected
206 because it is typically used to determine sedimentation for hindered settling (i.e.,
207 settling of intermediate concentrations of aggregates) (Verstraete and van Vaerenbergh,
208 1986). The sludge retention time (SRT) was not controlled and calculated based on the
209 ratio of total biomass in the reactor to the biomass flow in the effluent (Equation 1),
210 with Q representing the volumetric flow of the effluent, V the volume of the reactor and
211 C the biomass concentration in the reactor and the effluent. The SRT to HRT ratio
212 (SRT/HRT, unitless) was used as an indicator for biomass retention in the system.
213 Higher SRT to HRT ratios or improved biomass retention implies less sludge washout
214 due to better biomass aggregation and sedimentation.

$$215 \quad SRT = \frac{C_{biomass,in\ reactor} * V_{reactor}}{Q * C_{biomass,effluent}} \quad \text{Equation 1}$$

216

217 **3 Results and discussion**

218 **3.1 Operational strategies to enhance aggregation**

219 To analyze the influence of operational strategies on aggregation in PNSB,
220 different OLR and HRT were tested. First, a range of OLR (2-14.6 gCOD/(L.d)) and

221 HRT (0.3-0.04 d) was examined (section 3.1.1), as well as aggregation strategies at a
222 relative long HRT of 1 d (section 3.1.2).

223 **3.1.1 Organic loading rate and hydraulic retention time improve aggregation**

224 Both the OLR and the HRT affected PNSB aggregation in the upflow reactor
225 (Figure 2). Aggregation was highest at an OLR of 6.1 gCOD/(L.d) (HRT 0.1 d),
226 resulting in an average aggregation indicator (SRT/HRT ratio) of 90 ± 40 and a
227 sedimentation flux of 5.9 kgTSS/(m².h). Increasing the OLR to 14.6 gCOD/(L.d) (HRT
228 0.04 d), decreased the aggregation indicator to 62 ± 31 . Lowering the OLR to 2.0
229 gCOD/(L.d) (HRT 0.3 d), on the other hand, drastically decreased the aggregation
230 indicator to 10 ± 1 . Similar trends were observed by Driessens et al. (1987), where an
231 increase in OLR from 6.1 gCOD/(L.d) to 24.4 gCOD/(L.d) caused a decrease of the
232 aggregation indicator from 26 to 16, using a similar reactor setup and feed. The
233 sedimentation flux obtained by Driessens et al. (1987) at 6.1 gCOD/L was, however,
234 substantially lower (2 kgTSS/(m².h)) than what was achieved in this research (5.9
235 kgTSS/(m².h)).

236 Overall, COD removal efficiencies of $90 \pm 1\%$ were obtained. Only at the highest
237 OLR of 14.6 gCOD/(L.d) (HRT of 0.04 d), the COD removal efficiency decreased to 82
238 $\pm 6\%$, probably due to overloading of the system at shorter HRT (Alloul et al., 2019).

239 The effect of limited process parameters on PNSB aggregation has been studied
240 before. Apart from the research of Driessens et al. (1987), the influence of OLR and
241 HRT on aggregation of PNSB have not been studied. Stegman et al. (2021), testing
242 different upflow rates, reached an SRT/HRT ratio (aggregation indicator) of 15 in an
243 upflow reactor, lower than what was achieved in this research. The lower biomass

244 retention may be the result of higher hydrodynamic shear due to the higher upflow
245 velocity applied in the reactor (up to 9 m/h) (Tiwari et al., 2006). A sequencing batch
246 reactor with increasing OLR and decreasing HRT has also been used to aggregate
247 enriched PNSB, resulting in biomass with a sedimentation flux of 4.7 kgVSS/(m².h)
248 (Cerruti et al., 2020). In the studies of Cerruti et al. (2020) and Stegman et al. (2021)
249 however, both the OLR and HRT changed throughout the experiment, and the biomass
250 aggregation was only quantified at the end of the experiment, not at different OLR of
251 HRT.

252 For UASB reactors, it has been shown that HRT impacts the performance, yet
253 the organics to nitrogen ratio, micronutrients content, shear, upflow velocity, and type
254 of microorganisms are also crucial for aggregation (Tiwari et al., 2006). Typical HRT
255 used in UASB systems varies from 0.13 to 3 d with upflow rates ranging between 0.1
256 and 2 h/m (Khan et al., 2011; Latif et al., 2011). The OLR has also been shown to be an
257 important factor for aggregation in UASB reactors, as overloading the system can lead
258 to the accumulation of volatile fatty acids, due to activity of acidogenic fermentative
259 microorganisms, which can lower the reactor pH and negatively impact aggregation.
260 UASB systems are therefore typically operated at an OLR between 2 to 4.5 gCOD/(L.d)
261 (Tiwari et al., 2006). In this research, a high OLR did not impact the pH, but
262 concomitant shorter HRT may play a role in the reduced aggregation. Aerobic granular
263 sludge favors OLR between 0.5-10 gCOD/(L.d) and COD/N ratios between 2-30
264 gCOD/gN to maintain stable aggregates. Lower OLR or higher COD/N ratios can cause
265 disaggregation due to filamentous overgrowth. The HRT in these systems varies
266 between 0.17-1.0 d, as a consequence of the slow-growing microorganisms associated
267 with aerobic granular sludge (de Sousa Rollemberg et al., 2018).

268 **3.1.2 Improving aggregation at long hydraulic retention time in presence of**
269 **growth metabolites**

270 The previous section (3.1.1) showed that a relatively longer HRT (0.3 d) coupled
271 to a high OLR (14.6 gCOD/(L.d)) decreased aggregation of *Rb. capsulatus* biomass in
272 an anaerobic upflow reactor (Figure 2). In this section, only the effect of a long HRT
273 was examined by decoupling the OLR and HRT. The results in Figure 3A show that a
274 relatively longer HRT (while maintaining a constant OLR), results in a decline of the
275 aggregation indicator (SRT/HRT ratio) from 12 to 3 and COD removal efficiency from
276 97% to 87 %, indicating a decrease in biomass aggregation in the reactor. To avoid
277 disaggregation and washout of the biomass, tannic acid, a biological flocculant (Ge et
278 al., 2019; Wu et al., 2020), was added to the influent, which lead to a gradual recovery
279 and an increase of the aggregation indicator to 23 and COD removal efficiency to 91%.
280 These insights indicate that HRT control is essential for optimal aggregation. Similar
281 trends have been reported for aerobic flocs and aerobic granules, where a prolonged
282 HRT negatively affected the production of extracellular polymeric substances and
283 aggregation (Pan et al., 2004; Rosman et al., 2014; Trebuch et al., 2020).

284 The disaggregation at relatively long HRT was probably caused by the
285 accumulation of metabolites that hinder aggregation. This phenomenon is also observed
286 in other systems, where microalgae excrete organic matter, consisting out of a wide
287 range of polysaccharides, proteins, nucleic acids and more, which causes disaggregation
288 of the sludge bed (Pivokonsky et al., 2016). To explore whether accumulation of growth
289 metabolites caused disaggregation at high HRT, a pasteurization step was included in
290 the recirculation, since it was postulated that proportion of metabolites may be heat-
291 labile.

292 Pasteurization at 60 °C, 60-65 °C and 70-80 °C improved the aggregation
293 indicator from 3 to 6, 13 and 19 respectively, suggesting that the presence and
294 accumulation of heat-labile metabolites in the medium at higher HRT negatively impact
295 aggregation. The nature of the metabolites requires to be further determined, but these
296 observations indicate the importance of short HRT for aggregation of PNSB.

297 To study the effect of PNSB metabolites furthermore, supernatant from batch
298 cultures was fed in the reactor. After addition of supernatant, the aggregation indicator
299 (SRT/HRT ratio) abruptly decreased in the reactor (Figure 3B). Supernatant from 3-4
300 day old batch cultures showed a higher decrease in the aggregation indicator (from 21 to
301 5) than supernatant from 2-3 day old batch culture (aggregation indicator of 12).
302 Aggregation was reestablished when the reactor was switched to the original feed (data
303 not shown). Autoclaving the supernatant reversed this negative effect, improving
304 aggregation and increasing the aggregation indicator to 115. These observations indicate
305 the presence of a heat-labile metabolite in batch *Rb. capsulatus* cultures with the
306 potential to cause disaggregation.

307 **3.2 Wastewater characteristics influence aggregation**

308 To study the influence of wastewater composition on aggregation, different
309 COD/N ratios were tested (section 3.2.1) and the nitrogen source was changed from
310 ammonium to glutamate (section 3.2.2).

311 **3.2.1 Influence of the chemical oxygen demand to nitrogen ratio**

312 The composition of wastewater can vary depending on the source (Muys et al.,
313 2020) These differences create an imbalance in nutrient availability, which can cause a
314 shift in the metabolism and biomass composition (e.g. polyhydroxyalkanoate production

315 at high COD/N and polyphosphate accumulation at low COD/N) (Capson-Tojo et al.,
316 2020; Hiraishi and Kitamura, 1985). The impact of the COD/N ratio on PNSB
317 aggregation is, however, unknown. Therefore, investigating this factor creates a first
318 step in the transition to real wastewater. Both decreasing as increasing the COD/N ratio
319 showed improvement in the aggregation indicator (SRT/HRT ratio, 65 at 6 gCOD/gN,
320 47 at 12 gCOD/gN, 75 at 24 gCOD/gN). These findings were also confirmed with the
321 sedimentation fluxes (Figure 4A), making the COD/N ratio an important factor in PNSB
322 aggregation as well. For growth, an optimal influent COD/N around 16 gCOD/gN has
323 been found to prevent carbon or nitrogen limitations (Hülßen et al., 2014). Further
324 research should, however, clear out how this relates to the aggregation of PNSB.
325 Wastewater streams from plant-based food processing have overall a high COD/N ratio
326 (Verstraete et al., 2016), however, a pre-fermentation step can lower the COD content
327 (Alloul et al., 2018).

328 **3.2.2 Aggregation with organic nitrogen**

329 Apart from the COD/N ratio, the type of nitrogen source can also vary in
330 wastewater, yet the effect of nitrogen source has not been studied for PNSB
331 aggregation. Only ammonium has, thus far, been used as a nitrogen source (Cerruti et
332 al., 2020; Driessens et al., 1987; Stegman et al., 2021). PNSB metabolize both inorganic
333 and organic nitrogen sources, such as glutamate and yeast extract (Imhoff, 2006). The
334 nitrogen source was, therefore, changed to glutamate as an initial attempt to mimic the
335 complexity of real wastewater. At first, the aggregation index decreased at a COD/N
336 ratio of 35 gCOD/gN, indicating a disaggregation, however, the aggregation index
337 increased when the COD/N ratio was decreased to 22 gCOD/gN, restoring the
338 aggregation (Figure 4B). These trends were contrary to the results with ammonium

339 (section 3.2.1), where aggregation improved at a COD/N ratio of 24 gCOD/gN (Figure
340 4A). Aggregation with the organic nitrogen source was, consistently, inferior to
341 aggregation with inorganic nitrogen, as the sedimentation flux was 5.6 kgTSS/(m².h) for
342 ammonium at 24 gCOD/gN, and only 1.2 kgTSS/(m².h) for glutamate at 22 gCOD/gN.
343 The effect of organic nitrogen demands further investigation by selecting different N
344 sources (e.g., urea) and mixing inorganic and organic nitrogen, to mimic real
345 wastewater.

346 **3.3 Future perspectives**

347 Although certain operational approaches to affect PNSB aggregation have been
348 explored, some parameters have not been studied. The temperature of the incoming
349 wastewater, for example, can vary depending on the type and treatment stage.
350 Furthermore, for UASB systems, the pH has an impact on aggregation (Tiwari et al.,
351 2006), yet only a constant temperature was used in this experiment, as well as a constant
352 influent pH. Both temperature and pH, however, can affect flocculation of
353 photosynthetic bacteria (Lu et al., 2019) and could influence aggregation in the upflow
354 reactor. Apart from operational tools, more research needs to be done on scale-up of the
355 upflow photobioreactors, as sufficient illumination is necessary for phototrophic
356 growth. Granulation of the biomass enables more light penetration into the reactor,
357 compared to non-aggregated cells in suspension (Fradinho et al., 2021), however, only
358 the biomass on the surface of the aggregates is illuminated. The research of Cerruti et al.
359 (2020) shows that the microbial community is homogenous throughout the granules due
360 to the fast growth of PNSB, yet, nothing is known on the impact on the distribution of
361 the microbial community in the granules over a longer period.

362

363 **4 Conclusions**

364 The PNSB model organism *Rb. capsulatus* showed the best aggregation in an
365 upflow photobioreactor at OLR of 6.1 gCOD/(L.d) and HRT of 0.1 d, reaching a
366 sedimentation rate of 5.9 kgTSS/(m².h). Increasing the HRT did not improve
367 aggregation, possibly due to the accumulation of heat-labile metabolites interfering with
368 aggregation. Results indicate that wastewater streams with inorganic nitrogen and either
369 high or low COD/N ratios are better suited for aggregation. In addition, wastewater with
370 a low COD content is preferred, as this allows to maintain a short HRT without
371 overloading the system.

372

373 E-supplementary data for this work can be found in e-version of this paper
374 online

375

376 **Acknowledgments**

377 The authors kindly acknowledge (i) the project 'Saraswati 2.0' (821427) funded by the
378 European Union's Horizon 2020 Research and Innovation programme, for financial
379 support of A.A., (ii) the project 'PurpleRace' (40207) funded by IOF (Industrieel
380 onderzoeksfonds) from the University of Antwerp for financial support of A.A and
381 N.B., (iii) the Research Foundation Flanders (Fonds Wetenschappelijk Onderzoek -
382 Vlaanderen) for supporting A.A. with a postdoctoral fellowship (12W0522N).

383

384 **References**

- 385 1. Alloul, A., Ganigué, R., Spiller, M., Meerburg, F., Cagnetta, C., Rabaey, K.,
386 Vlaeminck, S.E., 2018. Capture-Ferment-Upgrade: A Three-Step Approach for the
387 Valorization of Sewage Organics as Commodities. *Environmental Science and*
388 *Technology* 52, 6729–6742. <https://doi.org/10.1021/acs.est.7b05712>
- 389 2. Alloul, A., Wille, M., Lucenti, P., Bossier, P., van Stappen, G., Vlaeminck, S.E.,
390 2021. Purple bacteria as added-value protein ingredient in shrimp feed: *Penaeus*
391 *vannamei* growth performance, and tolerance against *Vibrio* and ammonia stress.
392 *Aquaculture* 530. <https://doi.org/10.1016/j.aquaculture.2020.735788>
- 393 3. Alloul, A., Wuyts, S., Lebeer, S., Vlaeminck, S.E., 2019. Volatile fatty acids
394 impacting phototrophic growth kinetics of purple bacteria: Paving the way for
395 protein production on fermented wastewater. *Water Research* 152, 138–147.
396 <https://doi.org/https://doi.org/10.1016/j.watres.2018.12.025>
- 397 4. Bertanza, G., Canato, M., Laera, G., Vaccari, M., Svanström, M., Heimersson, S.,
398 2017. A comparison between two full-scale MBR and CAS municipal wastewater
399 treatment plants: techno-economic-environmental assessment. *Environmental*
400 *Science and Pollution Research* 24, 17383–17393. [https://doi.org/10.1007/s11356-](https://doi.org/10.1007/s11356-017-9409-3)
401 [017-9409-3](https://doi.org/10.1007/s11356-017-9409-3)
- 402 5. Capson-Tojo, G., Batstone, D.J., Grassino, M., Vlaeminck, S.E., Puyol, D.,
403 Verstraete, W., Kleerebezem, R., Oehmen, A., Ghimire, A., Pikaar, I., Lema, J.M.,
404 Hülsen, T., 2020. Purple phototrophic bacteria for resource recovery: Challenges
405 and opportunities. *Biotechnology Advances*.
406 <https://doi.org/10.1016/j.biotechadv.2020.107567>

- 407 6. CEC (Council of the European Communities), 1991. Council Directive of May
408 1991 concerning urban waste water treatment (91/271/EEC)., *Official Journal of*
409 *the European Communities*.
- 410 7. Cerruti, M., Stevens, B., Ebrahimi, S., Alloul, A., Vlaeminck, S.E., Weissbrodt,
411 D.G., 2020. Enrichment and Aggregation of Purple Non-sulfur Bacteria in a
412 Mixed-Culture Sequencing-Batch Photobioreactor for Biological Nutrient
413 Removal From Wastewater. *Frontiers in Bioengineering and Biotechnology* 8.
414 <https://doi.org/10.3389/fbioe.2020.557234>
- 415 8. de Sousa Rollemberg, S.L., Mendes Barros, A.R., Milen Firmino, P.I., Bezerra dos
416 Santos, A., 2018. Aerobic granular sludge: Cultivation parameters and removal
417 mechanisms. *Bioresource Technology*.
418 <https://doi.org/10.1016/j.biortech.2018.08.130>
- 419 9. Driessens, K., Liessens, J., Masduki, S., Verstraete, W., Nelis, H., 1987.
420 Production of *Rhodobacter capsulatus* ATCC 23782 with short residence time in a
421 continuous flow photobioreactor. *Process Biochemistry* 22, 160–164.
- 422 10. Fradinho, J., Allegue, L.D., Ventura, M., Melero, J.A., Reis, M.A.M., Puyol, D.,
423 2021. Up-scale challenges on biopolymer production from waste streams by
424 Purple Phototrophic Bacteria mixed cultures: A critical review. *Bioresource*
425 *Technology*. <https://doi.org/10.1016/j.biortech.2021.124820>
- 426 11. Gao, D., Liu, L., Liang, H., Wu, W.M., 2011. Aerobic granular sludge:
427 Characterization, mechanism of granulation and application to wastewater
428 treatment. *Critical Reviews in Biotechnology*.
429 <https://doi.org/10.3109/07388551.2010.497961>

- 430 12. Ge, D., Yuan, H., Xiao, J., Zhu, N., 2019. Insight into the enhanced sludge
431 dewaterability by tannic acid conditioning and pH regulation. *Science of the Total*
432 *Environment* 679, 298–306. <https://doi.org/10.1016/j.scitotenv.2019.05.060>
- 433 13. Hülsen, T., Batstone, D.J., Keller, J., 2014. Phototrophic bacteria for nutrient
434 recovery from domestic wastewater. *Water Research* 50, 18–26.
435 <https://doi.org/https://doi.org/10.1016/j.watres.2013.10.051>
- 436 14. Imhoff, J.F., 2006. The Phototrophic Alpha-Proteobacteria, in: *The Prokaryotes*.
437 *Springer New York*, 41–64. https://doi.org/10.1007/0-387-30745-1_2
- 438 15. Khan, A.A., Gaur, R.Z., Tyagi, V.K., Khursheed, A., Lew, B., Mehrotra, I.,
439 Kazmi, A.A., 2011. Sustainable options of post treatment of UASB effluent
440 treating sewage: A review. *Resources, Conservation and Recycling*.
441 <https://doi.org/10.1016/j.resconrec.2011.05.017>
- 442 16. Krishna, C., van Loosdrecht, M.C.M., 1999. Effect of temperature on storage
443 polymers and settleability of activated sludge. *Water Research* 33, 2374–2382.
- 444 17. Latif, M.A., Ghufuran, R., Wahid, Z.A., Ahmad, A., 2011. Integrated application of
445 upflow anaerobic sludge blanket reactor for the treatment of wastewaters. *Water*
446 *Research*. <https://doi.org/10.1016/j.watres.2011.05.049>
- 447 18. Lim, S.J., Kim, T.H., 2014. Applicability and trends of anaerobic granular sludge
448 treatment processes. *Biomass and Bioenergy*.
449 <https://doi.org/10.1016/j.biombioe.2013.11.011>
- 450 19. Liu, Y., Xu, H.-L., Yang, S.-F., Tay, J.-H., 2003. Mechanisms and models for
451 anaerobic granulation in upflow anaerobic sludge blanket reactor, *Water Research*.

- 452 20. Lu, H., Dong, S., Zhang, G., Han, T., Zhang, Y., Li, B., 2019. Enhancing the auto-
453 flocculation of photosynthetic bacteria to realize biomass recovery in brewery
454 wastewater treatment. *Environmental Technology (United Kingdom)* 40, 2147–
455 2156. <https://doi.org/10.1080/09593330.2018.1439107>
- 456 21. Mata-Alvarez, J., 2003. Fundamentals of the anaerobic digestion process.
457 Biomethanization of the organic fraction of municipal solid wastes 1–20.
- 458 22. Metcalf, L., Eddy, H.P., Tchobanoglous, G., 1991. Wastewater engineering:
459 treatment, disposal, and reuse. *McGraw-Hill New York*.
- 460 23. Monroy, I., Buitrón, G., 2020. Production of polyhydroxybutyrate by pure and
461 mixed cultures of purple non-sulfur bacteria: A review. *Journal of Biotechnology*
462 317, 39–47. <https://doi.org/https://doi.org/10.1016/j.jbiotec.2020.04.012>
- 463 24. Morgan-Sagastume, F., Allen, D.G., 2005. Physicochemical properties and
464 stability of activated sludge flocs under temperature upshifts from 30 to 45 C.
465 *Journal of colloid and interface science* 281, 136–145.
- 466 25. Muys, M., Papini, G., Spiller, M., Sakarika, M., Schwaiger, B., Lesueur, C.,
467 Vermeir, P., Vlaeminck, S.E., 2020. Dried aerobic heterotrophic bacteria from
468 treatment of food and beverage effluents: Screening of correlations between
469 operation parameters and microbial protein quality. *Bioresource Technology* 307,
470 123242. <https://doi.org/https://doi.org/10.1016/j.biortech.2020.123242>
- 471 26. Pan, S., Tay, J.-H., He, Y.-X., Tay, S.T.-L., 2004. The effect of hydraulic retention
472 time on the stability of aerobically grown microbial granules. *Letters in Applied*
473 *Microbiology* 38, 158–163. [https://doi.org/https://doi.org/10.1111/j.1472-](https://doi.org/https://doi.org/10.1111/j.1472-765X.2003.01479.x)
474 [765X.2003.01479.x](https://doi.org/https://doi.org/10.1111/j.1472-765X.2003.01479.x)

- 475 27. Rosman, N.H., Nor Anuar, A., Chelliapan, S., Md Din, M.F., Ujang, Z., 2014.
476 Characteristics and performance of aerobic granular sludge treating rubber
477 wastewater at different hydraulic retention time. *Bioresource Technology* 161,
478 155–161. <https://doi.org/https://doi.org/10.1016/j.biortech.2014.03.047>
- 479 28. Sakarika, M., Spanoghe, J., Sui, Y., Wambacq, E., Grunert, O., Haesaert, G.,
480 Spiller, M., Vlaeminck, S.E., 2020. Purple non-sulphur bacteria and plant
481 production: benefits for fertilization, stress resistance and the environment.
482 *Microbial Biotechnology* 13, 1336–1365.
483 <https://doi.org/https://doi.org/10.1111/1751-7915.13474>
- 484 29. Segers, L., Verstraete, W., 1983. Conversion of Organic Acids to H₂ by
485 Rhodospirillaceae Grown with Glutamate or Dinitrogen as Nitrogen Source.
486 *Biotechnology and Bioengineering* 25, 2843–2853.
487 <https://doi.org/https://doi.org/10.1002/bit.260251203>
- 488 30. Stegman, S., Batstone, D.J., Rozendal, R., Jensen, P.D., Hülsen, T., 2021. Purple
489 phototrophic bacteria granules under high and low upflow velocities. *Water*
490 *Research* 190. <https://doi.org/10.1016/j.watres.2020.116760>
- 491 31. Suresh, A., Grygolowicz-Pawlak, E., Pathak, S., Poh, L.S., Abdul Majid, M. bin,
492 Dominiak, D., Bugge, T.V., Gao, X., Ng, W.J., 2018. Understanding and
493 optimization of the flocculation process in biological wastewater treatment
494 processes: A review. *Chemosphere*.
495 <https://doi.org/10.1016/j.chemosphere.2018.07.021>

- 496 32. Tiwari, M.K., Guha, S., Harendranath, C.S., Tripathi, S., 2006. Influence of
497 extrinsic factors on granulation in UASB reactor. *Applied Microbiology and*
498 *Biotechnology*. <https://doi.org/10.1007/s00253-006-0397-3>
- 499 33. Trebuch, L.M., Oyserman, B.O., Janssen, M., Wijffels, R.H., Vet, L.E.M.,
500 Fernandes, T. v, 2020. Impact of hydraulic retention time on community assembly
501 and function of photogranules for wastewater treatment. *Water Research* 173,
502 115506. <https://doi.org/10.1016/j.watres.2020.115506>
- 503 34. Verstraete, W., Clauwaert, P., Vlaeminck, S.E., 2016. Used water and nutrients:
504 Recovery perspectives in a ‘panta rhei’ context. *Bioresour Technol* 215,
505 199–208. <https://doi.org/10.1016/j.biortech.2016.04.094>
- 506 35. Verstraete, W., van Vaerenbergh, E., 1986. Aerobic Activated Sludge .
507 *Biotechnology* 8, 43–112.
- 508 36. Verstraete, W., van Vaerenbergh, E., Bruyneel, B., Poels, J., Gellens, V.,
509 Grusenmeyer, S., Top, E., 1984. Biotechnological processes in environmental
510 technology. Laboratory General and Applied Microbial Ecology, State University
511 of Gent 352.
- 512 37. Wu, B., Dai, X., Chai, X., 2020. Critical review on dewatering of sewage sludge:
513 Influential mechanism, conditioning technologies and implications to sludge re-
514 utilizations. *Water Research*. <https://doi.org/10.1016/j.watres.2020.115912>

515

516

517

518 **Figure captions**

519 **Table 1.** Objectives and operational conditions for aggregation in a non-axenic upflow
520 photobioreactor inoculated with a pure *Rhodobacter capsulatus* ATCC 23782 culture.
521 HRT: hydraulic retention time, OLR: organic loading rate, COD: chemical oxygen
522 demand.

523 **Figure 1.** Configuration of the anaerobic upflow photobioreactor for aggregation of
524 purple non-sulfur bacteria, with an illuminated volume of 440 mL, and a decanter on
525 top. The reactor was inoculated with a pure culture of *Rhodobacter capsulatus* ATCC
526 23782 and operated non-axenically.

527 **Figure 2.** Conversion, aggregation and sedimentation features in an anaerobic upflow
528 photobioreactor inoculated with *Rhodobacter capsulatus* ATCC 23782. Panel A.
529 Influence of organic loading rate (OLR) on the aggregation indicator (sludge to
530 hydraulic retention time ratio SRT/HRT) and chemical oxygen demand (COD) removal
531 efficiency. OLR was controlled by varying the HRT. The decrease of the aggregation
532 index at day 5 is due to a measurement error. Panel B. The sedimentation fluxes of
533 aggregated biomass at HRT 0.1 d and HRT 0.04 d, determined for different dilutions of
534 aggregated biomass (no settling observed at HRT of 0.3 d).

535 **Figure 3.** Conversion and aggregation features in an anaerobic upflow photobioreactor
536 inoculated with *Rhodobacter capsulatus* ATCC 23782. Panel A. Influence of a long
537 hydraulic retention time (HRT 1 d) and addition of tannic acid on the aggregation
538 indicator (sludge retention time to hydraulic retention time ratio, SRT/HRT) and
539 chemical oxygen demand (COD) removal efficiency of aggregated biomass. Panel B.

540 Influence of addition of supernatant on the aggregation indicator and chemical oxygen
541 demand (COD) removal efficiency of aggregated biomass.

542 **Figure 4.** Sedimentation, conversion and aggregation features in an anaerobic upflow
543 photobioreactor inoculated with *Rhodobacter capsulatus* ATCC 23782. Panel A. The
544 sedimentation fluxes of aggregated biomass at COD/N ratio of 6, 12 and 24 gCOD/gN
545 with ammonium as nitrogen source, determined for four different dilutions of
546 aggregated biomass. Panel B. Influence of an organic nitrogen (glutamate) on the
547 aggregation indicator (sludge retention time to hydraulic retention time ratio SRT/HRT)
548 and chemical oxygen demand (COD) removal efficiency grown at COD/N ratios of 35
549 and 22 gCOD/gN with glutamate as nitrogen (and partial COD) source.

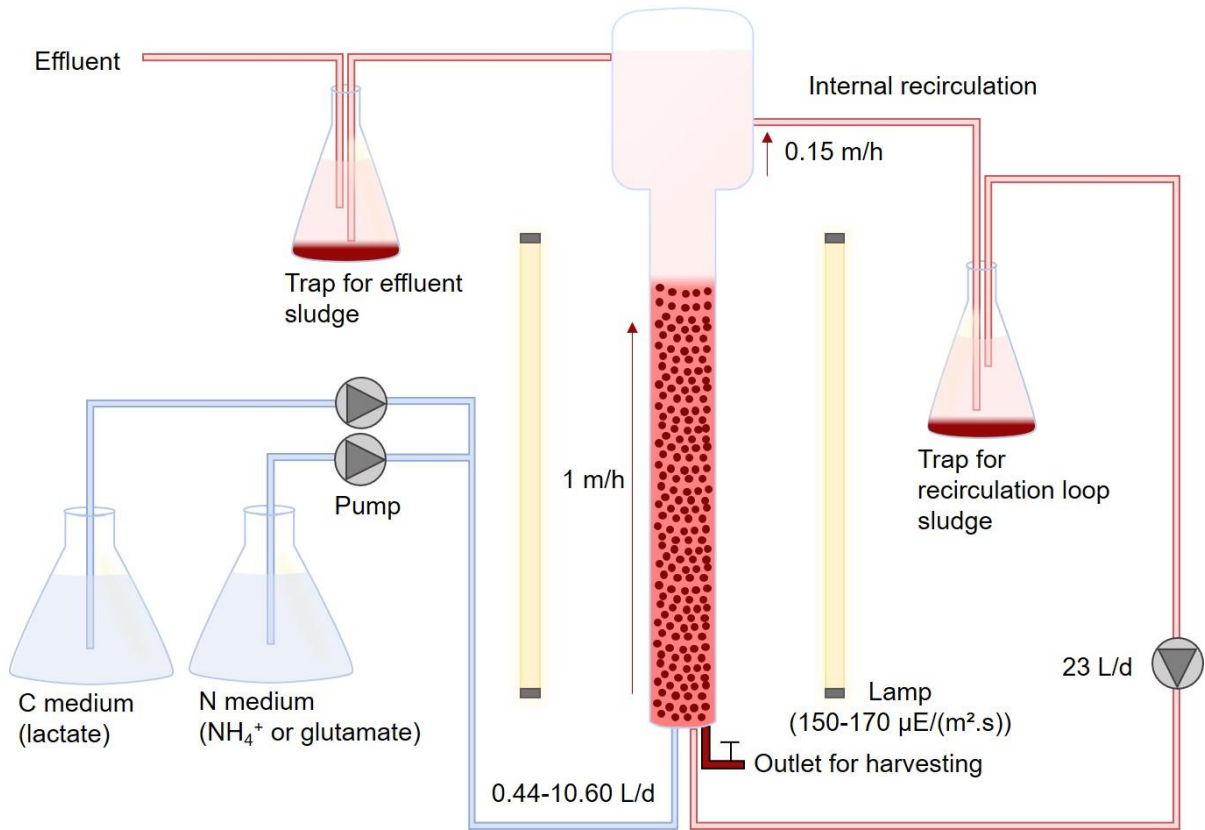
550

551 **Tables and figures**

552 Table 1.

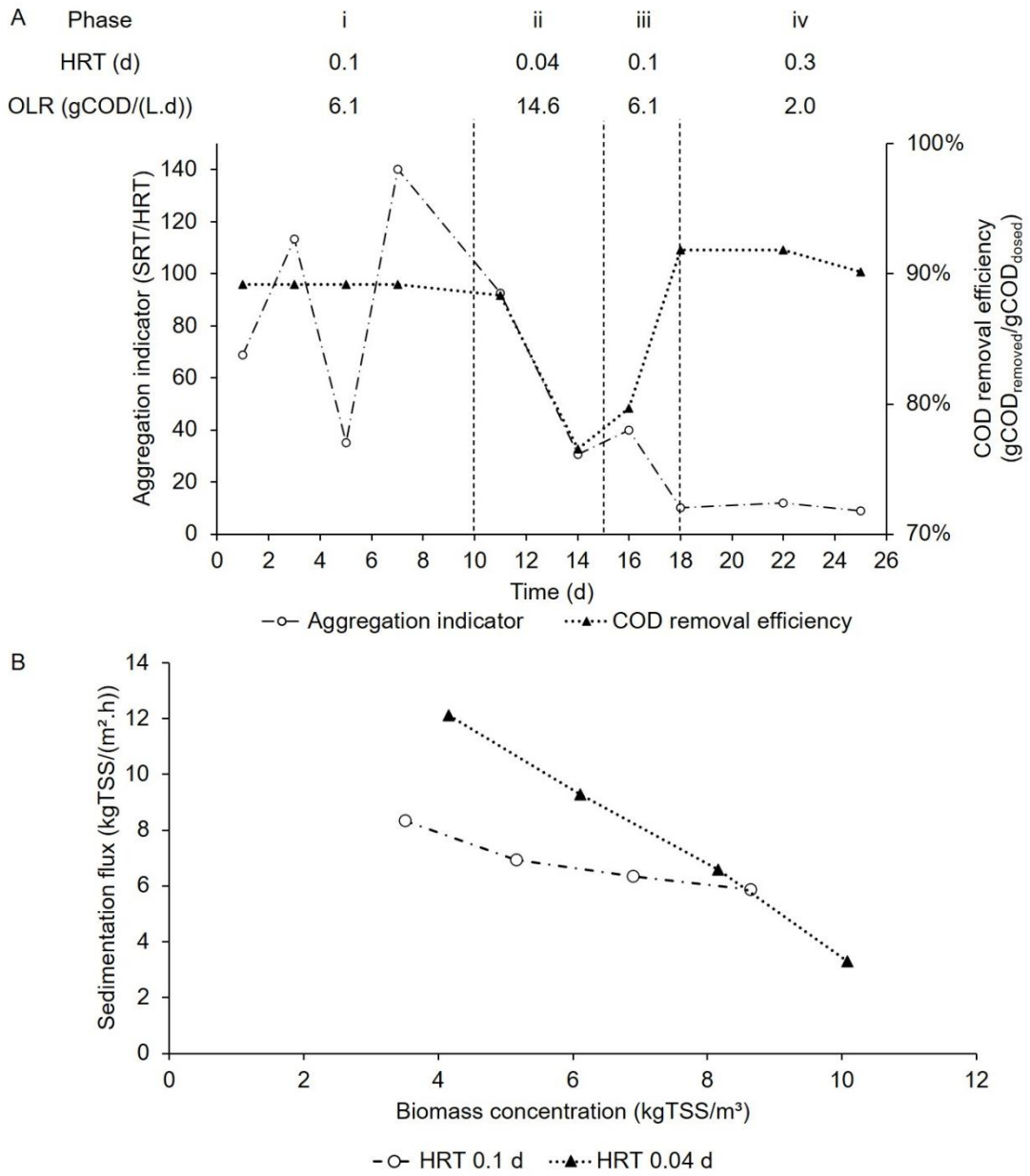
<i>Objective</i>	<i>HRT (d)</i>	<i>OLR (gCOD/(L.d))</i>	<i>COD/N (gCOD/gN)</i>	<i>Nitrogen source</i>	<i>Remarks</i>
Influence of OLR and HRT	0.04	14.6	12	Ammonium	
	0.1	6.1			
	0.3	2.0			
Aggregation at long HRT	1	12.2	12	Ammonium	Addition of tannic acid
		6.1			Pasteurization in the recirculation loop
Influence of COD/N ratio	0.1	3.0	6	Ammonium	
		6.1	12		
		12.2	24		
Influence of N source	0.1	8.6	22	Glutamate	
		11.1	35		
		12.2	12		
Influence of metabolites	0.1	12.2	12	Ammonium	Addition of supernatant from axenic batch cultures

553



554

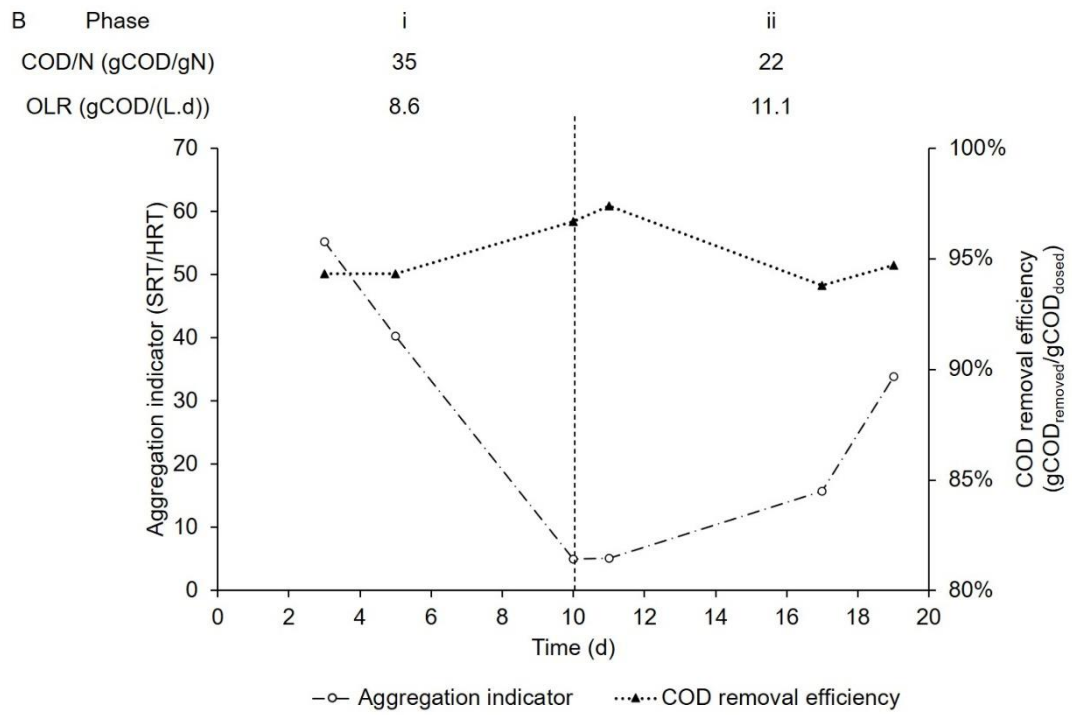
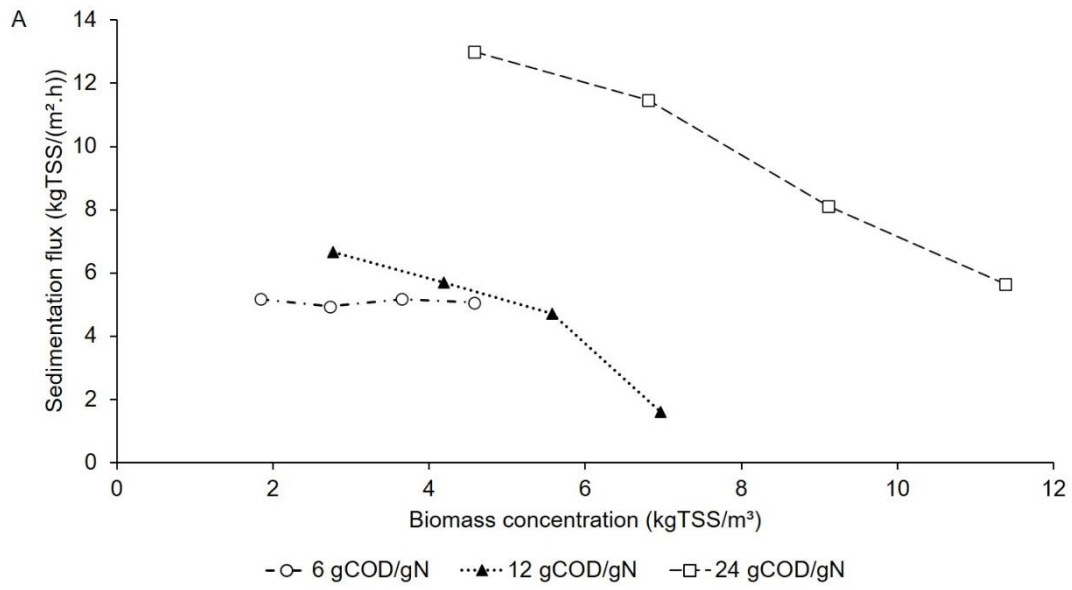
555 Figure 1



556

557 Figure 2

558



562

563 Figure 4

564